Applied Catalysis B: Environmental 165 (2015) 636–641

Contents lists available at ScienceDirect

Applied Catalysis B: Environmental

journal homepage: www.elsevier.com/locate/apcatb

A bimetallic carbide Fe_2MoC promoted Pd electrocatalyst with performance superior to Pt/C towards the oxygen reduction reaction in acidic media

Zaoxue Yan [a,*], Mingmei Zhang [a], Jimin Xie [a], Jianjun Zhu [a], Pei Kang Shen [b,*]

[a] School of Chemistry and Chemical Engineering, Jiangsu University, Zhenjiang, 212013, PR China
[b] State Key Laboratory of Optoelectronic Materials and Technologies, School of Physics and Engineering, Sun Yat-sen University, Guangzhou, 510275, PR China

ARTICLE INFO

Article history:
Received 14 August 2014
Received in revised form 3 October 2014
Accepted 28 October 2014
Available online 3 November 2014

Keywords:
Bimetallic carbide Fe_2MoC
Palladium electrocatalyst
Oxygen reduction reaction
Synergistic effect
Electrocatalysis

ABSTRACT

Novel and stable bimetallic carbide (Fe_2MoC) anchored on graphitized carbon (GC) has been synthesized by an ion-exchange method. The Pd supported on GC-Fe_2MoC electrocatalyst (Pd/GC-Fe_2MoC) shows superior activity and stability to commercial Pt/C for oxygen reduction reaction (ORR) in acidic media. The XPS spectra reveal that the excellent performance of Pd/GC-Fe_2MoC should be due to the excellent electron-donating (synergistic effect) of Fe_2MoC to Pd, which not only facilitates the reduction of O_2 but also increases the linkage strength between Pd and Fe_2MoC. The Koutecky-Levich plots indicate 4-electron transfer for the Pd/GC-Fe_2MoC catalyzed ORR.

1. Introduction

Transition metal carbides are effective to promote the noble metal based electrocatalysts because of their synergistic effect on noble metals. The synergistic effect is caused by the electron transfer between the carbides and noble metals [1–4], which well facilitates not only the oxidation of fuels and CO-like poisons [5–9], but also the reduction of oxygen (ORR) [10–15]. Therefore, with the combination of carbides and noble metals, great improvements in electrocatalytic activity in both anode and cathode have been obtained. However, the ORR performance still remains low in present due to slow kinetics [16,17], which needs large amount of Pt metal to improve the cathode current, leading to higher cost.

Palladium (Pd) has been proposed as a potential candidate for cathode electrocatalysts, due to their inherent catalytic activity and low cost compared with Pt. Pd-based electrocatalysts have good ORR performance in alkaline media [18–20]. However, the activity of Pd-based electrocatalysts towards ORR in acidic media is still lower than that of the Pt-based electrocatalysts [21–25]. Recently, bimetallic carbides ($Co_6Mo_6C_2$ [26] and Co_3W_3C [27]) have shown to be highly active and stable for promoting Pt- or Pd-based electrocatalysts towards ORR in acidic media, which are imagined to boom the study of bimetallic carbides.

Herein, we report novel bimetallic carbide composite (GC-Fe_2MoC), which comprises Fe_2MoC and graphitized carbon (GC, as matrix). The GC-Fe_2MoC promoted Pd electrocatalyst (Pd/GC-Fe_2MoC) exhibited higher activity and stability compared with commercial Pt/C towards ORR in acidic media. It has been realized that is due to the electron-donating effect (synergistic effect) and the inherent stability of Fe_2MoC.

2. Experimental

2.1. Preparation of GC-Fe_2MoC and GC-MoC composites

Typically, polyacrylic weak-base anion exchange resin (D314, 10 g, Shanghai Hualing Resin CO., Ltd, China) was firstly impregnated with 100 ml 0.014 mol L^{-1} ammonium molybdate ($(NH_4)_6Mo_7O_{24}$, A.R., Chemical Reagent Factory of Hefei University of Technology, China) for 6 h, then, the solid was separated and impregnated with 100 ml 0.200 mol L^{-1} potassium ferrocyanide ($K_4[Fe(CN)_6]$, A.R., Guangzhou Chemical Reagent Co., China) for 4 h. The resulting solid product was separated and dried at 80 °C overnight. Then, the product was heated at 1300 °C for 1 h in N_2

* Corresponding authors. Tel.: +86 20 84036736; fax: +86 20 84113369.
E-mail addresses: yanzaoxue@163.com (Z. Yan), stsspk@mail.sysu.edu.cn (P.K. Shen).

http://dx.doi.org/10.1016/j.apcatb.2014.10.070
0926-3373/

atmosphere. After cooled down to room temperature, the sample was grinded into powder by ball mill to get the GC-Fe_2MoC composite.

For comparison, the GC-MoC (MoC on graphitized carbon) was prepared. The preparation procedure is similar to that of GC-Fe_2MoC without the adding of $K_4[Fe(CN)]_6$.

2.2. Preparation of electrocatalysts

Pd supported on GC-Fe_2MoC was prepared. Typically, GC-Fe_2MoC (50 mg) was added into a mixture of 55.56 mg Palladium chloride ($PdCl_2$, A. R., Sinopharm Chemical Reagent Co., Ltd) and 20 ml glycol (A.R., Tianjin Fuyu Fine Chemicals Co., Ltd, China) in ultrasonic bath for 30 min to form a uniform ink. The pH of the mixture was adjusted to 10 by 1 mol L^{-1} NaOH/glycol solution. The sample was then put into a microwave oven (900 W) for heating at a 15 s on and 10 s off procedure for 10 times [28]. Afterwards, the mixture was washed with deionized water and dried in vacuum at 60 °C for 8 h to get the Pd/GC-Fe_2MoC electrocatalyst. The Pd content in the electrocatalyst was 40 wt% stoichiometrically. The actual Pd contents were determined by inductively coupled plasma-atomic emission spectrometry (ICP, IRIS(HR), USA).

For comparison, Pd/GC-MoC and Pd/C electrocatalysts with equivalent content of Pd were also synthesized.

2.3. Preparation of electrodes

For electrode preparation, Pd/GC-Fe_2MoC (or Pd/GC-MoC, Pd/C and GC-Fe_2MoC, 5 mg) or commercial Pt/C (4 mg, 47.6 wt %Pt, TKK, Japan) were dispersed in 1.95 ml ethanol and 0.05 ml 5 wt% Nafion suspension (DuPont, USA) under ultrasonic agitation to form the electrocatalyst ink. The electrocatalyst ink (0.005 ml) was deposited on the surface of a glass carbon rotating disk electrode (0.25 cm^2) and dried at room temperature. The total Pd or Pt loadings were all 0.02 mg cm^{-2}. The actual Pd or Pt content was determined by Inductively Coupled Plasma-atomic Emission Spectrometry (ICP, IRIS(HR), USA) method.

2.4. Electrochemical characterization

The electrochemical measurements were performed on a PARSTAT 2273 instrument in a three-electrode cell in an O_2-saturated 0.1 mol L^{-1} $HClO_4$ solution scanned between 0.03 to 1.1 V at a scan rate of 5 mV s^{-1}, at 25 °C controlled by a water-bath thermostat. A Pt foil (1.0 cm^2) and a reversible hydrogen electrode (RHE) were used as counter and reference electrodes, respectively.

All chemicals were of analytical grade and used as received.

2.5. Physical characterization

The morphologies of the synthesized materials were characterized by transmission electron microscopy (TEM, JOEP JEM-2010, JEOL Ltd.) operating at 200 kV. The graphitization degrees were determined with Laser Micro-Raman Spectrometer (Renishaw inVia, Renishaw plc). The structures of the samples were determined on an X-ray diffractometer (XRD, D/Max-IIIA, Rigaku Co., Japan, CuK1, $\lambda = 1.54056$ Å radiation) and an X-ray Photoelectron Spectroscopy (XPS, ESCALAB 250, Thermo-VG Scientific).

3. Results and discussion

Fig. 1 shows the XRD patterns of the GC-Fe_2MoC and GC-MoC composites. The patterns of GC-Fe_2MoC and GC-MoC composites match the characteristics of Fe_2MoC (PDF#17-0911) and MoC (PDF#65-0280) respectively by comparing JCPDS cards. Besides, the diffraction peaks at 2θ around 26.0° correspond to C (0 0 2) facet of

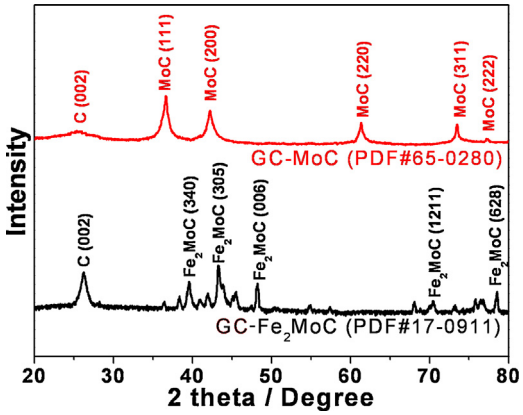

Fig. 1. XRD patterns of GC-Fe_2MoC and GC-MoC composites.

graphite. But it is apparent that GC-Fe_2MoC has more graphitization degree than GC-MoC. Literatures reported that Fe compound as graphitization catalyst leads to graphitization of organics by a complex process involving the dissolution of carbon atoms into catalyst followed by the precipitation of graphitized carbon [29–31]. Above results proved that the addition of Fe compound lead to high graphitization degree of the GC-Fe_2MoC. Meanwhile, the Fe compound also acts as a reagent leading to the formation of Fe_2MoC.

Fig. 2 shows the Raman spectra of GC-Fe_2MoC and GC-MoC composites. The G peaks at 1598 cm^{-1} for GC-MoC and at 1580 cm^{-1} for GC-Fe_2MoC correspond to a splitting of the E2g stretching mode of graphite and reflects the structural intensity of the sp^2-hybridized carbon atom [32,33]. The positive shift on GC-MoC compared to that on GC-Fe_2MoC means the inferior graphite orientation of the former than that of the latter. The D peak at 1350 cm^{-1} is attributed to the vibrations of carbon atoms with dangling bonds in disordered graphite planes and the defects incorporated into pentagon and heptagon graphite-like structures. The ratios of the G-line to D-line were used to determine the degree of the graphitization. The I_G/I_D values for GC-Fe_2MoC and GC-MoC were 2.46 and 1.21, respectively. These results confirm that the Fe compound favors the graphitization of D314 resin, leading to higher graphitization degree of GC-Fe_2MoC.

Fig. 3a is the TEM image of the GC-Fe_2MoC. The particles with the diameter ranged from 5 to 15 nm are uniformly dispersed. From the HRTEM image (Fig. 3b), the lattices of the Fe_2MoC (3 0 5) and graphite (0 0 2) can be clearly seen. Fig. 3c is the TEM image of Pd/GC-Fe_2MoC, the particles with the diameter of no more than 5 nm and with the diameter around 10 nm should be

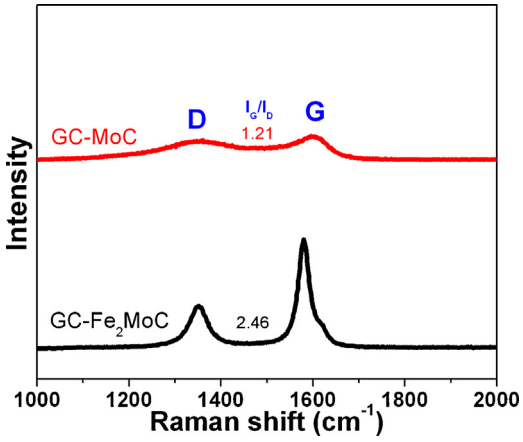

Fig. 2. Raman spectra of GC-Fe_2MoC and GC-MoC composites.

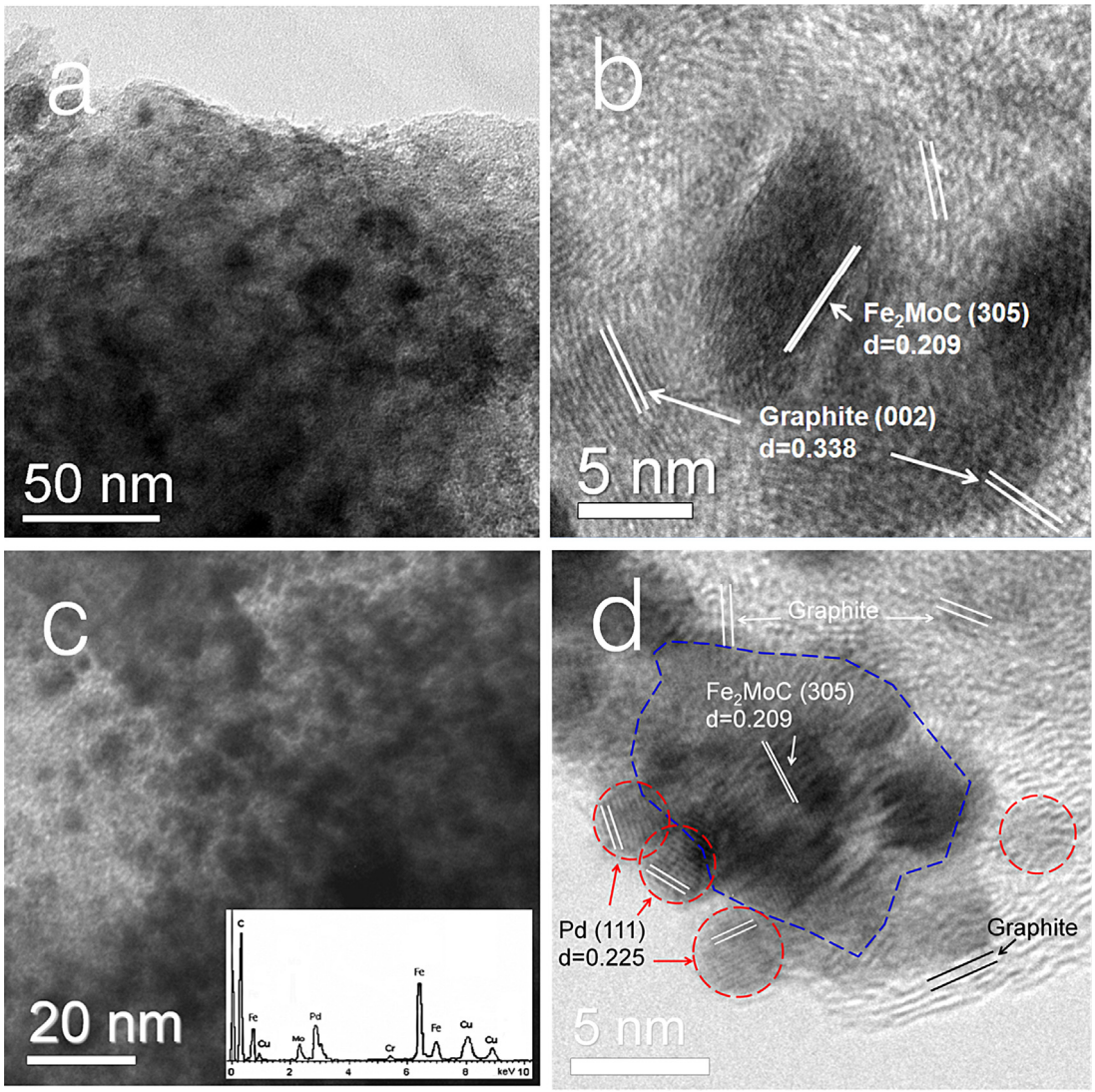

Fig. 3. (a) TEM and (b) HRTEM images of GC-Fe_2MoC, (c) TEM and (d) HRTEM images of Pd/GC-Fe_2MoC. Inset of (c) is the corresponding EDS pattern.

mainly correspond to the Pd and Fe_2MoC. The corresponding EDS pattern (inset of Fig. 3c) proves the coexistence of Pd, Fe, Mo and C elements (the peaks of Cu and Cr elements come from the sample bracket). Fig. 3d is the HRTEM image of Pd/GC-Fe_2MoC, which clearly shows the lattices of Fe_2MoC (3 0 5), graphite C (0 0 2) and Pd (1 1 1) facets. It also can be seen that Pd nanoparticles are closely around or on surface of the Fe_2MoC nanoparticles, which are imagined to produce well synergistic effect between them when being used in electrocatalysis. In addition, the graphite as support is imagined to improve the electrical conductivity and electrochemical stability compared to amorphous carbon [34,35]. As to the GC-MoC composite, the structures with the similar synthesis had been reported in details in literature [36].

Fig. 4 shows the XRD patterns of Pd/GC-Fe_2MoC, Pd/GC-MoC and Pd/C. The peaks of Pd obviously existed in all three samples with the peaks of MoC and Fe_2MoC. From the peak shape of Pd, it can be proximately judged that all three samples have the similar Pd particle size.

The ORR performances of the Pd/GC-Fe_2MoC, Pd/GC-MoC, Pd/C, GC-Fe_2MoC and Pt/C electrodes were determined in O_2-saturated 0.1 mol L^{-1} $HClO_4$ solution at 25 °C with the scan rate of 5 mV s^{-1}, 1600 rpm, as shown in Fig. 5. The electrodes all have the same Pd or Pt loadings of 0.02 mg cm^{-2}. It can be seen from Fig. 5a that the onset potential of these electrocatalysts is in the following order: commercial Pt/C (+1.03 V) = Pd/GC-Fe_2MoC (+1.03 V) > Pd/GC-MoC (+0.96 V) > Pd/C (+0.93 V) > GC-Fe_2MoC (+0.79 V). The half-potential ($E_{1/2}$) values of these electrocatalysts are in the following order:

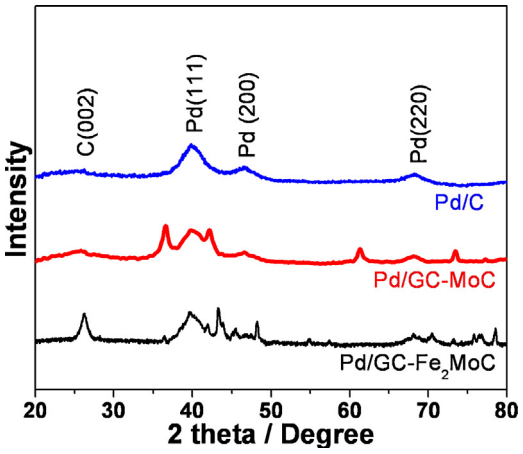

Fig. 4. XRD patterns of Pd/GC-Fe_2MoC, Pd/GC-MoC and Pd/C.

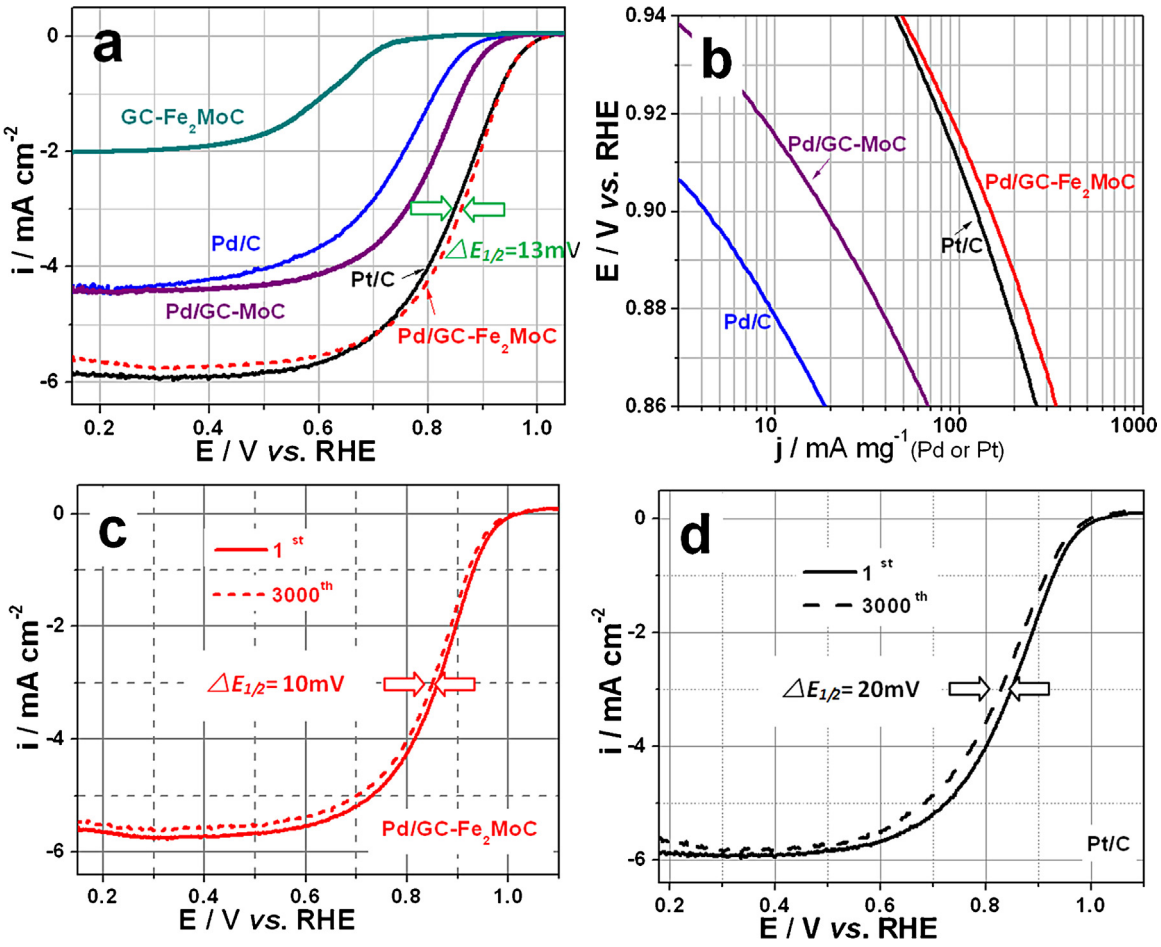

Fig. 5. (a) ORR curves, (b) the corresponding mass activities of the electrocatalysts at the 1st cycles, (c) and (d) ORR curves of the Pd/GC-Fe_2MoC and commercial Pt/C electrocatalysts at the 1st and 3000th cycles. The ORR was performed in O_2-saturated 0.1 mol L^{-1} $HClO_4$ solution at 25 °C with the scan rate of 5 mV s^{-1}, 1600 rpm.

Pd/GC-Fe_2MoC (+0.86 V) > commercial Pt/C (+0.85 V) > Pd/GC-MoC (+0.76 V) > Pd/C (+0.69 V). The $E_{1/2}$ value of ORR on the Pd/GC-MoC electrocatalyst is approximately 70 mV more positive than that of the Pd/C electrocatalyst, indicating that the introduction of graphite and MoC to the Pd electrocatalyst significantly reduces the ORR overpotential. More significantly, the $E_{1/2}$ value of ORR on the Pd/GC-Fe_2MoC electrocatalyst is approximately 170 mV more positive than that of the Pd/C electrocatalyst. The reduction in overpotential is believed mainly due to the electron-donating from MoC or Fe_2MoC to Pd, which favors the reduction of O_2. In addition, the graphitized carbon as support has higher electrical conductivity than amorphous carbon [34], which would further reduce the ORR overpotential on Pd/GC-MoC and Pd/GC-Fe_2MoC. The electron-donating from MoC or Fe_2MoC to Pd will be proved by performing XPS characterization.

Fig. 5b shows the kinetic currents of the electrocatalysts calculated from the experimental data using the mass transport correction for rotating disk electrode [37]:

$$i_k = i_d i/(i_d - i) \quad (1)$$

where i is the experimentally obtained current, i_d refers to the measured diffusion-limited current and i_k the mass-transport-free kinetic current. The mass activity (i_m) can be determined via the calculation of i_k using Eq. (1) and normalized to the Pd or Pt loadings. The mass activities at +0.9 V of these electrocatalysts were measured and summarized in Table 1. It can be seen that the mass activities of the electrocatalysts are in the following order: Pd/GC-Fe_2MoC (146.4 mA mg^{-1} Pd) > commercial Pt/C (124.3 mA mg^{-1} Pt) > Pd/GC-MoC (18.7 mA mg^{-1} Pd) > Pd/C (4.2 mA mg^{-1} Pd). The results proved that the Pd/GC-Fe_2MoC exhibits much higher ORR activity than that of the commercial Pd/C electrocatalyst and superior to Pt/C as well in acidic media.

To evaluate the stability of the Pd/GC-Fe_2MoC electrocatalyst, the ORR curves for Pd/GC-Fe_2MoC and commercial Pt/C in the 1st and 3000th cycles were compared in an O_2-saturated 0.1 mol L^{-1} $HClO_4$ solution. After 3000th cycle, the $E_{1/2}$ values decreased 10 mV for Pd/GC-Fe_2MoC (Fig. 5c) and 20 mV for commercial Pt/C (Fig. 5d), respectively. The mass activities at +0.9 V of the two

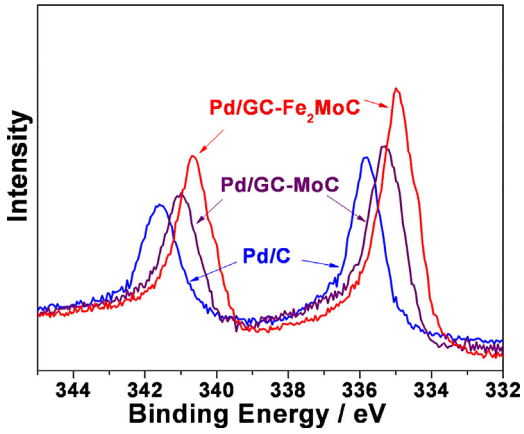

Fig. 6. XPS spectra (Pd 3d) of Pd/GC-Fe_2MoC, Pd/GC-MoC and Pd/C.

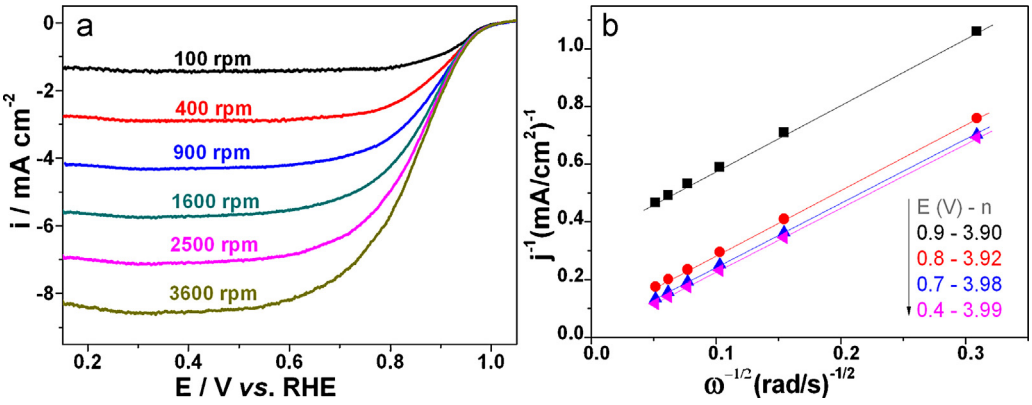

Fig. 7. (a) The ORR curves on Pd/GC-Fe_2MoC catalyst at different rotating speeds in O_2-saturated 0.1 mol L^{-1} $HClO_4$ solution at 25 °C with the scan rate of 5 mV s^{-1} and (b) the corresponding Koutecky-Levich plots at different potentials (the number of electrons transferred is marked).

Table 1
The mass activities of the four electrocatalysts.

Electrocatalyst	Pd or Pt mass content	i_m at 0.9 V (mA $mg^{-1}_{(Pd\ or\ Pt)}$)		Activity retention
		1st cycle	3000th cycle	
Pd/GC-Fe_2MoC	37.6%	146.4	118.1	80.7%
Pd/GC-MoC	37.7%	18.7	–	–
Pd/C	38.2%	4.2	–	–
Pt/C	47.6%	124.3	86.8	69.8%

electrocatalysts were calculated according to Eq. (1) and also summarized in Table 1. It was found that the activity retention of 80.7% was achieved for the Pd/GC-Fe_2MoC electrocatalyst, while, it was only 69.8% for the commercial Pt/C electrocatalyst. This finding indicated that the Pd/GC-Fe_2MoC has an excellent stability comparable to that of $Pt/Co_6Mo_6C_2$ [26].

The XPS spectra (Pd 3d) of Pd/GC-Fe_2MoC, Pd/GC-MoC and Pd/C are presented in Fig. 6, which can be use to explain the electrocatalyst performances. The XPS spectra show that the Pd/GC-Fe_2MoC and Pd/GC-MoC material exhibited a 0.9 eV and a 0.5 eV decrease in electron binding energy compared with that of Pd/C materials, indicating electron-donating (transfer) from Fe_2MoC and MoC to metallic Pd, which favors the reduction of O_2. The results are similar with the synergistic effect of carbides on noble metals [8]. It is notable that the Fe_2MoC has more degree of electron-donating compared to that of MoC, indicating more promotion of Fe_2MoC than MoC on Pd electrocatalyst activity, which account for the less overpotential and higher mass activity of Pd/GC-Fe_2MoC, as discussed above. On the other hand, the more degree of electron transfer means the higher linkage between Pd and Fe_2MoC, which may account for the excellent electrocatalytic stability of Pd/GC-Fe_2MoC.

Fig. 7a shows the ORR curves on Pd/GC-Fe_2MoC at the rotating speeds of 100, 400, 900, 1600, 2500 and 3600 rpm respectively. The transferred electron number (n) per oxygen molecule involved can be calculated on the basis of the Koutecky-Levich equation (2) [38–40]:

$$\frac{1}{j} = \frac{1}{j_K} + \frac{1}{0.62nFAC_{O_2}D_{O_2}^{2/3}\nu^{-1/6}\omega^{1/2}} \quad (2)$$

where j is the measured current density (mA cm^{-2}), j_k is the kinetic current density of the ORR, n is the overall number of electrons transferred during the oxygen reduction, F is the Faraday constant (96485 C mol^{-1}), C is the bulk concentration of O_2 (1.22×10^{-3} mol L^{-1}), D_{O2} is the diffusion coefficient of O_2 in 0.1 mol L^{-1} $HClO_4$ electrolyte (1.9×10^{-5} cm^2 s^{-1}), ν is the kinetic viscosity of the electrolyte (9.97×10^{-3} cm^2 s^{-1}), and ω is the angular velocity of the disk ($\omega = 2\pi \times$ rpm/60 rad s^{-1}, where rpm is the linear rotation speed). The j^{-1} plotted against the $\omega^{-1/2}$ resulting in Koutecky-Levich plots at the typical potentials of 0.9, 0.8, 0.7 and 0.4 V respectively are shown in Fig. 7b. The number of electrons transferred (n) calculated according to Koutecky-Levich Eq. (2) is also marked in Fig. 7b. It can be seen that the ORR catalyzed by Pd/GC-Fe_2MoC has 3.90, 3.92, 3.98 and 3.99 electrons transferred at the potentials of 0.9, 0.8, 0.7 and 0.4 V respectively, indicating a direct 4-electron reduction of O_2 to H_2O on Pt/GC-Fe_2MoC, which is more efficient than that of the Pt/C catalyst reported in literature [41].

4. Conclusions

A stable structured novel bimetallic carbide (Fe_2MoC) promoted Pd electrocatalyst for the ORR in acidic media has been developed. The Pd/GC-Fe_2MoC electrocatalyst showed much higher activity than that of Pd/C and even superior to Pt/C in O_2-saturated 0.1 mol L^{-1} $HClO_4$ solution, making it a promising platinum-free acidic ORR electrocatalyst. The origin of the excellent performance of Pd/GC-Fe_2MoC should be mainly due to the inherent stability of Fe_2MoC and its electron-donating (synergistic effect) to Pd, which not only improved the activity by facilitating the reduction of O_2, but also improve the stability by increasing the linkage strength between Pd and Fe_2MoC. In addition, the graphitized carbon with high graphitization degree may also improve the activity and stability due to high electrical conductivity and high chemical inertia [42].

Acknowledgements

This work was funded by China Postdoctoral Science Foundation (2014T70481), National Natural Science Foundations of China (21306067, 21073241), Natural Science Foundations of Jiangsu (BK20130490, BK20140531), the link project of the National Natural Science Foundation of China and Guangdong Province (U1034003), the Major International (Regional) Joint Research Project (51210002) and the Industry High Technology Foundation of Jiangsu (BE2013090).

References

[1] H. Meng, P.K. Shen, Chem. Commun. (2005) 4408–4410.
[2] J. Yang, Y. Xie, R. Wang, B. Jiang, C. Tian, G. Mu, J. Yin, B. Wang, H. Fu, ACS Appl. Mater. Inter. 5 (2013) 6571–6579.
[3] K.G. Nishanth, P. Sridhar, S. Pitchumani, A.K. Shukla, Fuel Cells 12 (2012) 146–152.
[4] M.D. Obradovi, B.M. Babi, V.R. Radmilovi, N.V. Krstaji, S.L. Gojkovi, Int J. Hydrogen Energ. (2012) 10671–10679.

[5] R. Wang, J. Yang, K. Shi, B. Wang, L. Wang, G. Tian, B. Bateer, C. Tian, P. Shen, H. Fu, RSC Adv. 3 (2013) 4771–4777.
[6] C. Ma, L. Kang, M. Shi, X. Lang, Y. Jiang, J. Alloy. Compd. 588 (2014) 481–487.
[7] M. Yin, Q. Li, J.O. Jensen, Y. Huang, L.N. Cleemann, N.J. Bjerrum, W. Xing, J. Power Sources 219 (2012) 106–111.
[8] G. Cu, P.K. Shen, H. Meng, J. Zhao, G. Wu, J. Power Sources 196 (2011) 6125–6130.
[9] Z. Fu, Q.M. Huang, X.D. Xiang, Y.L. Lin, W. Wu, S.J. Hu, W.S. Li, Int J. Hydrogen Energ. 37 (2012) 4704–4709.
[10] Y. Wang, S. Song, V. Maragou, P.K. Shen, P. Tsiakaras, Appl. Catal. B-Environ. 89 (2009) 223–228.
[11] A.C. Garcia, E.A. Ticianelli, Electrochim. Acta 106 (2013) 453–459.
[12] I.J. Hsu, Y.C. Kimmel, Y. Dai, S. Chen, J.G. Chen, J. Power Sources 199 (2012) 46–52.
[13] C. Liang, L. Ding, C. Li, M. Pang, D. Su, W. Li, Y. Wang, Energ. Environ. Sci. 3 (2010) 1121–1127.
[14] V. Kiran, K. Srinivasu, S. Sampath, Phys. Chem. Chem. Phys. 15 (2013) 8744.
[15] T. Huang, S. Mao, H. Pu, Z. Wen, X. Huang, S. Ci, J. Chen, J. Mater. Chem. A 1 (2013) 13404–13410.
[16] N.R. Elezović, B.M. Babić, L. Gajić-Krstajić, P. Ercius, V.R. Radmilović, N.V. Krstajić, L.M. Vračar, Electrochim. Acta 69 (2012) 239–246.
[17] Y. Liu, T.G. Kelly, J.G. Chen, W.E. Mustain, ACS Catal. 3 (2013) 1184–1194.
[18] Y.W. Lee, A.R. Ko, S.B. Han, H.S. Kim, D.Y. Kim, S.J. Kim, K.W. Park, Chem. Commun. 46 (2010) 9241–9243.
[19] Y.H. Xue, L. Zhang, W.J. Zhou, S.H. Chan, Int. J. Hydrogen Energ. 39 (2014) 8449–8456.
[20] R.C. Sekol, X. Li, P. Cohen, G. Doubek, M. Carmo, A.D. Taylor, Appl. Catal. B-Environ. 138–139 (2013) 285–293.
[21] K. Oishi, O. Savadogo, J. Electroanal. Chem. 703 (2013) 108–116.
[22] C.L. Lee, H.P. Chiou, Appl. Catal. B-Environ. 117–118 (2012) 204–211.
[23] R. Carrera-Cerritos, V. Baglio, A.S. Aricò, J. Ledesma-García, M.F. Sgroi, D. Pullini, A.J. Pruna, D.B. Mataix, R. Fuentes-Ramírez, L.G. Arriaga, Appl. Catal. B-Environ. 144 (2014) 554–560.
[24] J.H. Shim, J. Kim, C. Lee, Y. Lee, Chem. Mater. 23 (2011) 4694–4700.
[25] S. Yin, M. Cai, C. Wang, P.K. Shen, Energ. Environ. Sci. 4 (2011) 558–563.
[26] X. Ma, H. Meng, M. Cai, P.K. Shen, J. Am. Chem. Soc. 134 (2012) 1954–1957.
[27] Z. Li, S. Ji, B.G. Pollet, P.K. Shen, Chem. Commun. 50 (2014) 566–568.
[28] Z.Q. Tian, S.P. Jiang, Y.M. Liang, P.K. Shen, J. Phys. Chem. B 110 (2006) 5343–5350.
[29] F.J. Maldonado-Hódar, C. Moreno-Castilla, J. Rivera-Utrilla, Y. Hanzawa, Y. Yamada, Langmuir 16 (2000) 4367–4373.
[30] L. Wang, C. Tian, B. Wang, R. Wang, W. Zhou, H. Fu, Chem. Commun. (2008) 5411–5413.
[31] Z. Yan, G. He, M. Cai, H. Meng, P.K. Shen, J. Power Sources 242 (2013) 817–823.
[32] M.S. Dresselhaus, G. Dresselhaus, R. Saito, A. Jorio, Phys. Rep. 409 (2005) 47–99.
[33] T. Belin, F. Epron, Mater. Sci. Eng. B 119 (2005) 105–118.
[34] Z. Yan, M. Cai, P.K. Shen, J. Mater. Chem. 22 (2012) 2133–2139.
[35] Z. Yan, M. Zhang, J. Xie, P.K. Shen, J. Power Sources 243 (2013) 336–342.
[36] Z. Yan, G. He, P.K. Shen, Z. Luo, J. Xie, M. Chen, J. Mater. Chem. A 2 (2014) 4014–4022.
[37] B. Lim, M.J. Jiang, P.H.C. Camargo, E.C. Cho, J. Tao, X.M. Lu, Y.M. Zhu, Y.A. Xia, Science 324 (2009) 1302–1305.
[38] S. Štrbac, I. Srejić, M. Smiljanić, Z. Rakočević, J. Electroanal. Chem. 704 (2013) 24–31.
[39] J. Zagal, P. Bindra, E. Yeager, J. Electrochem. Soc. 127 (1980) 1506–1517.
[40] M.S. Ahmed, D. Kim, S. Jeon, Electrochim. Acta 92 (2013) 168–175.
[41] M. Ammam, E.B. Easton, J. Power Sources 236 (2013) 311–320.
[42] Z. Yan, H. Meng, P.K. Shen, R. Wang, L. Wang, K. Shi, H. Fu, J. Mater. Chem. 22 (2012) 5072–5079.